

CFD ANALYSIS ON SOLAR AIR HEATER WITH ARTIFICIAL ROUGHENED BROKEN CURVED RIBS

Kundan Kumar, Shivasheesh Kaushik, Vijay Singh Bisht

Abstract— Solar air heaters provides the efficient use of solar energy, which uses the absorber plate to absorb the incoming solar radiations, converting it to thermal energy at its surface, and transferring the thermal energy to the fluid flowing through the collector. It has been observed that the efficiency of the flat plate solar air heater is low because of low convective heat transfer coefficient between the absorber plate and the air flowing over it. The most common and effective way to improve the performance of the solar air heater is to provide artificial roughness elements on the underside of the absorber plate. This work is concerned with the CFD Analysis of Solar Air heater with artificial roughened broken curved ribs to predict convective heat transfer properties. Solar air heater is a useful device for extracting heat from solar energy. The Reynolds number (Re) range from 4000 to 20,000 for relative roughness height (e/D_h), relative roughness pitch 8 to 14, the angle of curve (α) in the range of 30° – 75° , hydraulic diameter 0.0333 meter and gap width $g/e=1$. The broken curved roughness on absorber plate of solar air heater with an aspect ratio of 5:1. The roughened absorber plate being heated while the remaining three walls are insulated. Computational fluid dynamics (CFD) simulations were performed using commercially available software ANSYS FLUENT 15.0. The effect of parameters on the heat transfer and friction are compared with the result of smooth duct under similar flow conditions.

Index Terms— Heat Transfer, Artificial Roughness, Solar Air Heater, Broken Curved Ribs, Ansys 14.5.

1 INTRODUCTION

As our non-renewable resources are set to decline in the years to come and global spike in energy costs has led many to find alternative and sustainable fuel sources. There are many options available today including wind, biogas, solar, hydro-power and tidal energy. Of these, solar is the fastest growing and almost everyone can learn to capture its power to perform tasks like cooking; lighting, heating, and many other household chores.

Solar air heater (SAHs) is a solar thermal technology in which solar energy is converted into thermal energy and further used for space heating ,drying laundry ,crop etc. SAH is generally used due to simple in design and low installation cost. But for conventional SAHs is low value of heat transfer coefficient between absorber plate and flowing fluid (air) and thermal efficiency is low in turbulent condition also because of a laminar sub-layer forms in turbulent boundary layer which adjacent to heat transferring surface of absorber plate. The laminar sub-layer grows in thickness along the flow direction as a result thermal performance of conventional SAHs is adversely affected. Various method is used for the thermal performance enhancement such as double pass, finned absorber, packed bed, periodic rib roughness etc in which periodic rib roughness method is most effective as it creates turbulence in a flow region near heat transferring surface of absorber plate where laminar sub-layer develops; and it does not affect the core flow due to which increase in pumping power requirements are less as compared to other performance enhancement

• Kundan Kumar, *Research Scholar in Department of Thermal Engineering, UTU (Uttarakhand Technical University) Dehradun, Uttarakhand, India ,PH-9897622826. E-mail: kundankmr79@gmail.com*

• Shivasheesh Kaushik, *Assistant Professor in Department of MECHANICAL Engineering, AGI (Amarpali Group of Institute) Haldwani, Uttarakhand, India ,PH-9756298215. E-mail: shivasheesh.rachit.kaushik@gmail.com*

• Vijay Singh Bisht, *Assistant Professor in Department of MECHANICAL Engineering, UTU (Uttarakhand Technical University) Dehradun, Uttarakhand, India ,PH-9012233525. E-mail: vsinghbisht5@gmail.com*

methods. Heat transfer and friction factor correlations for a solar air heater duct roughened artificially with broken arc ribs by v.s. Hans et al, In this experimental investigation, solar air heater duct with aspect ratio 12 roughened with broken arc rib has been investigated. To investigate the influence of roughness parameters of broken arc rib on Nusselt number as well as on friction factor the roughened plate having relative roughness pitch (P/e), relative gap width (g/e), relative gap position (d/w), relative roughness height (e/D_h) and arc angle (α) varying from 4-12, 0.5-2.5, 0.2-0.8, 0.022-0.043 and 15° - 75° respectively, have been investigated for Reynolds number range of 2000-16000. The maximum increase in Nusselt number and friction factor over that of continuous arc rib roughened duct was 1.19 and 1.14 times respectively. The corresponding values over that of smooth duct were 2.63 and 2.44 times respectively.

Numerical study on thermal hydraulic performance improvement in solar air heater duct with semi ellipse shaped obstacles by tabish alam, This paper presents numerical study on heat transfer and friction characteristics in rectangular solar air heater duct with semi elliptical shape obstacles. 3-D simulations have been conducted using Renormalization-group $k-\epsilon$ turbulence model. Obstacles are placed on the absorber plate in V-down shape at different angle of attack (α), ranging from 30° to 90° . Two different arrangements of obstacles namely; inline and staggered arrangements have been investigated. Four different values of Reynolds number, ranging from 6000 to 18,000 have been considered to determine the values of Nusselt number and friction factor. Angle of attack (α) and obstacles arrangement significantly affect the Nusselt number and friction factor. In staggered arrangement, maximum enhancement in Nusselt number and friction factor have been observed 2.05 and 6.93, respectively, at an angle of attack (α) of 75° and corresponding enhancement in case of inline arrangement are found as 1.73 and 6.12, respectively. The maximum enhancement in Nusselt number at 75° angle of attack is due to combined effect of high turbulence and lateral movement of air flow. Thermo hydraulic performance has also been

determined which shows staggered arrangement are more superior than inline arrangement for all values of angle of attack (α) investigated in present study.

A critical review on artificial roughness provided in rectangular solar air heater duct by tabish alam, Applications of artificial roughness on the underside of absorber plate in solar air heater duct have been widely used to improve heat transfer with moderate increase of friction factor. The design of the roughness shape and arrangement is most important to optimize the roughened surfaces. The roughness parameters and ribs arrangement are responsible to alter the flow structure and heat transfer mechanisms are mainly governed by flow structure. The critical reviews on various artificial roughness elements available in literature have been conducted and the effects of the roughness patterns are discussed. The Nusselt number and friction factor correlations for various roughness elements have been summarized. A comparison study of thermo hydraulic performance of different roughness elements has also been reported to understand the results of applications of artificial roughness.

Performance Evaluation of Solar Air Heater With Novel Hyperbolic Rib Geometry Deep Singh Thakur et al[4] ; In this CFD analysis for the evaluation of thermo-hydraulic performance of artificially roughened solar air heater's absorber plate with novel hyperbolic ribs of roughness height (e) from 0.5 mm to 2 mm and pitch (P) from 10 mm to 20 mm. The optimum performance is achieved for $e = 1$ mm and $P = 10$ mm at $Re = 6000$. The performance of this novel rib is compared with rectangular, triangular and semicircular rib geometries and is found to be the best among all up to $Re = 10000$.

A CFD based Thermo-Hydraulic Performance Analysis of an Artificially Roughened Solar Air Heater Having Circular Ribs on the Absorber Plate, Amit Kumar Ahuja et al[5] ; The thermo-hydraulic performance of artificial roughened solar absorber plate with Relative roughness pitch P/e 7.14-20 Relative roughness height e/D 0.03-0.042 Hydraulic diameter 33.33 Reynolds number Re 8000-180000 Uniform Heat flux I 1000 W/m^2 The average nusselt number increases with increase in

Reynolds number in all cases for fixed value of relative roughness height Maximum nusselt number has been found to be 2.223 times compared to smooth duct corresponds to relative roughness height (e/D) of 0.042 and relative roughness pitch (P/e) of 7.142 at Reynolds number 15000 in the range of parameter investigated.

Experimental investigation of heat transfer augmentation using multiple arcs with gap on absorber plate of solar air heater N.K. Pandey et al[6] The investigation encompassed Reynolds number (Re) ranges from 2100 to 21,000 (7 values), relative roughness height (e/D) ranges from 0.016 to 0.044 (4 values), relative roughness pitch (p/e) ranges from 4 to 16 (4 values), arc angle values are 30–75(4 values), relative roughness width (W/w) ranges from 1 to 7 (5 values), relative gap distance (d/x) values are 0.25–0.85 (4 values) and relative gap width (g/e) ranges from 0.5 to 2.0 (4 values). The maximum increment in Nusselt number (Nu) and friction factor (f) is 5.85 and 4.96 times in comparison to the smooth duct. The maximum enhancement for Nu takes place at Reynolds number (Re) value of 21,000, g/e value of 1, d/x value of 0.65, W/w value of 5, e/D value of 0.044, p/e value of 8 and $a/60$ value of 1.

Yadav and Bhagoria studied the effects of heat transfer and fluid flow characteristics in artificially roughened solar air heater using CFD. The effects of small diameter of transverse wire rib roughness on heat transfer and fluid flow have been investigated. The maximum value of average Nusselt number was found to be 117 for relative roughness pitch of 7.14 and for relative roughness height of 0.042 at a higher Reynolds number, 18,000. The maximum enhancement of average Nusselt number and frictional factor was found to be 2.31 and 0.0317 times that of smooth duct for relative roughness pitch of 7.14 and for relative roughness height of 0.042.

Raj Kumar et al study and correlation development correlation for Nusselt number and friction factor for discretized broken V-pattern baffle solar air channel. Experiments have been carried out for system parameter such as a width to height ratio, of 10, the relative baffle gap distance, range of 0.26-0.83, relative baffle gap width, range of 0.5-1.5, relative baffle height,

range of 0.25-0.80, relative baffle pitch, range of 0.5-2.5, and angle of attack, range of 30o-70o. The effect of discretized broken V-pattern baffle has been investigated for the range of Reynolds number from 3000 to 21000. The maximum enhancement is observed at a of 0.67, of 1.0, of 0.50, of 1.5, and of 60°.

2 OBJECTIVE

The main aim is to investigate the varying effects on heat transfer characteristics or parameters on solar air heater with artificial roughened broken curved ribs flow with varying mass flow rate and axial velocity. The other major objectives are as follows:

- 1- To calculate Nusselt number with varying mass flow rate for different spacing inserts.
- 2- To calculate friction factor with varying Reynolds number for different spacing inserts.
- 3- To calculate Pressure Drop with varying mass flow rate for different spacing inserts.
- 4- To calculate Average wall temperature with varying mass flow rate for different spacing inserts.
- 5- To develop various contours for optimum mass flow rate for different spacing inserts.

3 GOVERNING EQUATION

3.1 GOVERNING EQUATION

The behaviour of the flow is generally governed by the fundamental principles of the classical mechanics expressing the conservation of mass and momentum. Here the considered steady, incompressible, turbulent flow is modeled by the momentum and continuity equations. The continuity and the momentum equations are as follows.

3.1.1 CONTINUITY EQUATION

Continuity Equation also called conservation of mass. Consider fluid moves from point 1 to point 2. The overall mass bal-

ance is Input - output = accumulation. Assuming that there is no storage the Mass input = mass output. However, as long as the flow is steady (time-invariant), within this tube, since, mass cannot be created or destroyed then the above equation. According to continuity equation, the amount of fluid entering in certain volume leaves that volume or remains there and according to momentum equation tells about the balance of the momentum. The momentum equations are sometimes also referred as Navier-Stokes (NS) equation. They are most commonly used mathematical equations to describe flow. The simulation is done based on the NS equations and then K-Epsilon model. Continuity equation can be expressed as:

$$\frac{\delta(\rho\bar{u})}{\delta x} + \frac{1}{r} \frac{\delta(\rho r\bar{v})}{\delta r} = 0 \tag{3.1}$$

3.2 MOMENTUM EQUATION

3.2.1 AXIAL COMPONENT (Z-COMPONENT)

$$\rho\bar{v} \left[\frac{\delta\bar{u}}{\delta r} + \bar{u} \frac{\delta\bar{u}}{\delta x} \right] = \frac{\delta\bar{p}}{\delta x} + \frac{\delta}{\delta x} \left(\mu_{eff} \frac{\delta\bar{u}}{\delta x} \right) + \frac{1}{r} \frac{\delta}{\delta r} \left(r \mu_{eff} \frac{\delta\bar{u}}{\delta r} \right) + \frac{\delta}{\delta x} \left(\mu_{eff} \frac{\delta\bar{u}}{\delta x} \right) + \frac{1}{r} \frac{\delta}{\delta r} \left(\mu_{eff} \frac{\delta\bar{u}}{\delta r} \right) \tag{3.2}$$

3.2.2 RADIAL COMPONENT (R-COMPONENT)

$$\rho\bar{v} \left[\frac{\delta\bar{v}}{\delta r} + \bar{u} \frac{\delta\bar{v}}{\delta x} \right] = -\frac{\delta\bar{p}}{\delta r} + \frac{\delta}{\delta x} \left(\mu_{eff} \frac{\delta\bar{v}}{\delta x} \right) + \frac{1}{r} \frac{\delta}{\delta r} \left(r \mu_{eff} \frac{\delta\bar{v}}{\delta r} \right) + \frac{\delta}{\delta x} \left(\mu_{eff} \frac{\delta\bar{v}}{\delta x} \right) + \frac{1}{r} \frac{\delta}{\delta r} \left(r \mu_{eff} \frac{\delta\bar{v}}{\delta r} \right) - 2\mu_{eff} \frac{\bar{v}}{r^2} + \rho \frac{\bar{w}^2}{r} \tag{3.3}$$

3.2.3 TANGENTIAL COMPONENT (Θ- COMPONENT)

$$\rho \left[\bar{v} \frac{\delta\phi}{\delta r} + \bar{u} \frac{\delta\phi}{\delta x} \right] = \frac{\delta}{\delta x} \left[\mu_{eff} \frac{\delta\phi}{\delta x} \right] + \frac{1}{r} \frac{\delta}{\delta r} \left[r \mu_{eff} \frac{\delta\phi}{\delta r} \right] - \frac{2}{r} \frac{\delta}{\delta r} \left[\mu_{eff} \phi \right] \tag{3.4}$$

Here \bar{u} , \bar{v} and \bar{w} are the mean velocity components along z, r

and θ directions respectively and the variable $\phi = r\bar{w}$.

The total effective viscosity of the flow is given by,

$$\mu_{eff} = \mu_l + \mu_t \tag{3.5}$$

Here μ_l and μ_t stand for molecular or laminar vis-

cosity and eddy or turbulent viscosity respectively. The molecular or the laminar viscosity is the fluid property and the eddy viscosity or the turbulent viscosity is the flow property.

By using dimensional analysis, the eddy viscosity μ_t can be expressed as,

$$\mu_t = \rho V_t l \tag{3.6}$$

Here V_t , is the turbulent velocity scale and l is the turbulent length scale. It was postulated by Prandtl and Kolmogorov and later adopted in the standard k-ε model that

$$l = \frac{\kappa^{3/2}}{\epsilon} \tag{3.7}$$

$$V_t \sim \sqrt{k} \tag{3.8}$$

From the equation (3.6) the eddy viscosity is obtained and it is given by

$$\mu_t = \frac{\rho c \mu k^2}{\epsilon} \tag{3.9}$$

The modeling constant, C_μ in the eddy viscosity formulation, as shown in equation (3.10), is empirically tuned for the simple shear layer. The constant, C_μ is given by

$$C_\mu = \frac{-k_1 k_2}{\left[1 + 8 k_1^2 \frac{k^2}{\epsilon^2} \left(\frac{\delta U_s}{\delta r} + \frac{U_s}{R_c} \right) \frac{U_s}{R_c} \right]} \tag{3.10}$$

In the equation (3.10), $U_s = \sqrt{\bar{u}^2 + \bar{v}^2}$ and R_c is the radius of curvature of the streamline concerned (Ψ constant).

3.3 THE TURBULENT MODELING

3.3.1 KAPPA-EPSILON MODEL

The K-epsilon model is most commonly used to describe the behavior of turbulent flows. It was proposed by A.N Kolmogorov in 1942, then modified by Harlow and Nakayama and produced K-Epsilon model for turbulence. The Transport

Equations for K-Epsilon model are for k, Realizable k-epsilon model and RNG k-epsilon model are some other variants of K-epsilon model. K-epsilon model has solution in some special cases. K-epsilon model is only useful in regions with turbulent, high Reynolds number flow.

K – EQUATION

$$\rho [\bar{u} \frac{\partial k}{\partial x} + \bar{v} \frac{\partial k}{\partial r}] = \frac{\partial}{\partial x} [(\mu_l + \frac{\mu_t}{\sigma_k}) \frac{\partial k}{\partial x}] + \frac{1}{r} \frac{\partial}{\partial r} [r(\mu_l + \frac{\mu_t}{\sigma_k}) \frac{\partial k}{\partial r}] - \rho \epsilon \tag{3.11}$$

Where, G is the production term and is given by

$$\mu_t [2\{(\frac{\partial \bar{v}}{\partial r})^2 + (\frac{\partial \bar{u}}{\partial x})^2 + (\frac{\bar{v}}{r})^2\} + (\frac{\partial \bar{u}}{\partial r} + \frac{\partial \bar{v}}{\partial x})^2] \tag{3.12}$$

The production term represents the transfer of kinetic energy from the mean flow to the turbulent motion through the interaction between the turbulent fluctuations and the mean flow velocity gradients.

ε - EQUATION

$$\rho [\bar{u} \frac{\partial \epsilon}{\partial x} + \bar{v} \frac{\partial \epsilon}{\partial r}] = \frac{\partial}{\partial x} [(\mu_l + \frac{\mu_t}{\sigma_\epsilon}) \frac{\partial \epsilon}{\partial x}] + \frac{1}{r} \frac{\partial}{\partial r} (r\mu_l + \frac{\mu_t}{\sigma_\epsilon}) \frac{\partial \epsilon}{\partial r} + C_{s1} G \frac{\epsilon}{k} - C_{s2} \frac{\epsilon^2}{k} \tag{3.13}$$

Here C_{s1} , C_{s2} , σ_k and σ_ϵ are empirical turbulent constant. The values are considered according to the Launder, et. al.

3.4 PERFORMANCE PARAMETERS

This section describes how heat transfer and pressure drop are characterized. Included are dimensionless groups, equations for heat transfer and efficiency calculations, and equations for making pressure drop calculations. Following the descriptions of the performance parameters, the values as read from the graphs in the research done by Wang, et. al. (1996) for friction factor f and Colburn j-factor vs. Reynolds number.

3.4.1 DIMENSIONLESS GROUPS

Accurate characterisation of the flow friction and heat transfer

is very important in rating and sizing heat exchangers. Dimensional groups are used for this characterisation: heat transfer defined with the Colburn factor j and pressure drop defined by friction factor f. Below is a summary of the dimensionless groups used in this project, the equation to calculate it, and a brief description.

3.4.1.1 REYNOLDS NUMBER

The Reynolds number Re represents the ratio of flow inertial forces to viscous forces. The Reynold’s number characteristic dimension for this study is the tube collar diameter Dc.

$$Re = \frac{\rho \cdot U_i \cdot D_h}{\mu} \tag{3.14}$$

3.4.1.2 FRICTION FACTOR F

The Fanning friction factor is the ratio of wall shear stress to the flow kinetic energy. It is related to pressure drop tube heat exchangers as:

$$f = \frac{\Delta p \cdot \frac{D_h}{L_t}}{\frac{1}{2} \cdot \rho \cdot U_i^2} \tag{3.15}$$

Where Lt is length of duct,(m); ρ is air density (Kg/m^3); Δp is pressure drop (Pa).

3.4.1.3 COLBURN J-FACTOR

The Colburn j-factor is the ratio of convection heat transfer (per unit duct surface area) to the amount virtually transferable (per unit of cross-sectional flow area).

$$j = \frac{Nu}{Re_{D_c} \cdot Pr^{1/3}} \tag{3.16}$$

3.4.1.4 NUSSELT NUMBER Nu

The Nusselt number is the ratio of convective conductance h to molecular thermal conductance k/Dh.

$$Nu = \frac{h}{k / D_h} \tag{3.17}$$

The Nusselt number is based on the hydraulic diameter Dh.

$$D_h = \frac{4(F_p - t)(P_t - D_c)P_l}{2(P_l P_t - \pi D_c^2 / 4) + \pi D_c (F_p - t)} \quad (3.18)$$

3.4.1.5 PRANDTL NUMBER PR

The Prandtl number Pr is the ratio of a fluid's momentum diffusivity to thermal diffusivity.

$$Pr = \frac{\nu}{\alpha} = \frac{\mu C_p}{k} \quad (3.19)$$

3.4.1.6 PRESSURE DROP

The pressure drop determines the amount of pumping power needed to run a heat exchanger. It is therefore important to characterize the pressure drop for design. This section describes how the pressure drop relates to the pumping power, followed by a description of what causes the pressure drop and finally the pressure drop equations for tube-and-fin heat exchangers are presented as:

$$\Delta p = \frac{L}{D} \frac{\rho V^2}{2} \quad (3.20)$$

Pumping power P is often seen as an important design constraint because the pressure drop in a heat exchanger (along with associated pressure drops in the inlet/outlet headers, nozzles, ducts, etc.) is proportional to the amount of fluid pumping power needed for the heat exchanger to function, as given by the following expression.

4 GEOMETRICAL DISCRPTION

4.1 NUMERICAL SOLUTION PROCERSS

Due to the advances in computational hardware and available numerical methods, CFD is a powerful tool for the prediction of the fluid motion in various situations, thus, enabling a proper design. CFD is a sophisticated way to analyze not only for fluid flow behaviour but also the processes of heat and mass transfer. Advances in physical models, numerical analysis and computational power enable simulation of the heat transfer characteristics in three-dimensional circumstances. A

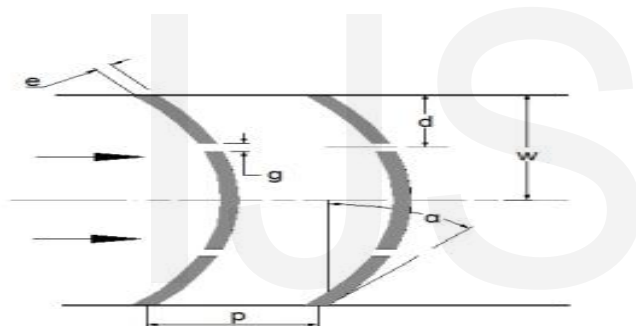
three dimensional approximation of a turbulent flow is chosen to explore since the three-dimensional approach is considerably greater than two dimensional and moreover, a turbulent flow is fundamentally three-dimensional. Owing to extremely long computation times, detailed studies on the fluid flow through pipes in three-dimensional flow are very uncommon. Hence, the simulation of the three-dimensional flow field under complex geometrical conditions is seemingly intricate and challenging task. The available computational fluid dynamics software package FLUENT is used to determine the related problems. FLUENT uses a finite volume method and requires from the user to supply the grid system, physical properties and the boundary conditions. When planning to simulate a problem, basic computation model considerations such as boundary conditions, the size of computational domain, grid topology, two dimensions or three-dimension model, are necessary. For example, appropriate choice of the grid type can save the set up time and computational expense. Moreover, a careful consideration for the selection of physical models and determination of the solution procedure will produce more efficient results. Dependent on the problem, the geometry can be created and meshed with a careful consideration on the size of the computational domain, and shape, density and smoothness of cells. Once a grid has been fed into FLUENT, check the grids and executes the solution after setting models, boundary conditions, and material properties. FLUENT provides the function for post processing the results and if necessary refined the grids is available and solve again as the above procedure. As described in the objective, the purpose of this study is to investigate numerically the effect of misdistribution in the solar air heater. The whole analysis is carried out with the help of software "ANSYS Fluent 15.0". ANSYS Fluent 15.0 is computational fluid dynamics (CFD) software package to stimulate fluid flow problems. The three dimensional computational domain modelled using tetrahedral mesh for 3-D models. The complete domain of 3-D duct in all cases have fix element size. Grid independence test was performed to check the validity of the quality of the mesh on the solution. Further refinement did

not change the result by more than 0.9% which is taken as the appropriate mesh quality for computation.

4.2 METHODOLOGY

The methodology of the present study can be divided into four stages of process flow which are geometry modeling, pre-processing, processing and post-processing. Various steps in adopted methods are:

- Mathematical modeling of the system considered in present study.
- Developed the model in SOLIDWORKS.
- Validation of present work with previous research.
- Calculation of heat transfer parameters.
- Run program to obtain the plots with different parameters.
- Plotting & analysis of obtained plots.



- Optimization of the system.

Figure 4.1: Parametric model of Broken Curved Ribs

Table number 4.1: The dimension of air heater geometry parameters

Heater type	Solar air heater having broken arc rib
Length	640 mm
Width	100 mm
Hight	20 mm
Arc angle (α)	30
Relative roughness pitch (p/e)	8 to 14
Relative roughness height (e/Dh)	0.045
Gap width (g/e)	1
Fluid	Air

4.3 SIMULATION OF FLOW THROUGH SOLAR AIR HEATER

For the CFD analysis of solar air heater first the fluid domain was designed using Solid works. The boundary conditions applied to the channel, the assumptions made, the equations used, the results obtained after calculation and then the results were analysed

4.4 GEOMETRICAL DESCRIPTION

Geometry of solar air heater was designed using solid works 2013. To see the fluid behaviour inside the channel. Corrugated shape was given to see the changes in heater. These geometrical models of plates are used for studying the effects of the variation of Reynolds number on the performance of heater.

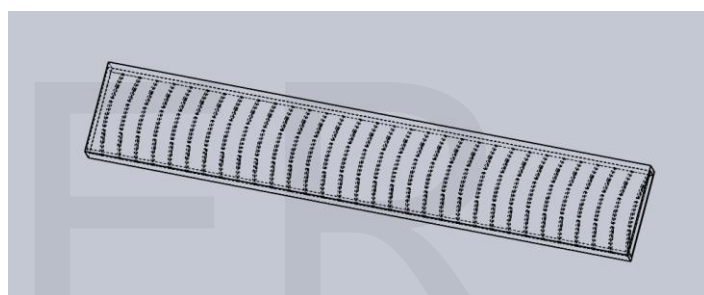


Figure 4.2: Geometry view of artificial roughness

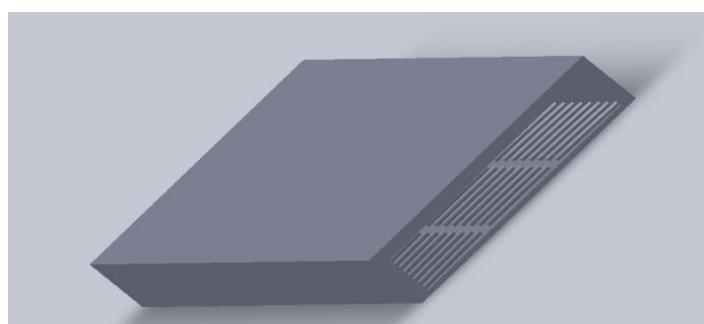


Figure 4.3: Geometry view of solar air heater model

5. RESULT AND DISCUSSION

In present work solar air heater is analysed for performance enhancement. Simple solar air heater and Solar air heater with triangular shape geometry inside the tube is analysed. CFD analysis of both design carried out in ANSYS Fluent 15. Different turbulence model are used and compared to see the difference for suitable results. Turbulence model are selected

based on the value of Nusselt number with respect to Reynolds number for both design. K-ε model (standard) and K-ε model RNG, K-ε model realizable model are used to verify the results. The Nusselt number obtained using Dittus-Boelter eq. for both design. As the result of turbulence models compare, K-ε turbulence RNG model is used to study the present work. Present numerical results are also validated with previous results. The present numerical result shows good agreement with previous results.

5.1 VALIDATION OF MODEL

In present work solar air heater is analysed for performance enhancement. Simple solar air heater and Solar air heater with triangular shape geometry inside the tube is analysed. CFD analysis of both design carried out in ANSYS Fluent 15.

5.1.1 GRID INDEPENDENCE TEST

For selection of mesh element count different no of mesh element size 265131, 871997, 1508485 and 2080414 are performed on smooth duct for nusselt no. at different Reynolds no. the value of Nusselt no. increases initially but after mesh element 1508485 the value of nusselt no. is constant so for calculation of nusselt number for smooth duct 1508485 mesh element is used.

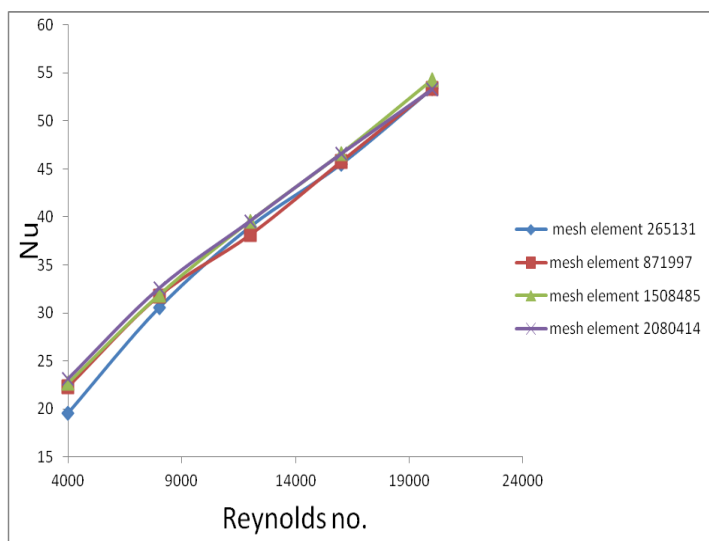


Fig. 4.1 Nusselt and Reynolds no. for different mesh element

5.1.2. SELECTION OF MODEL

For selection of turbulence model for smooth duct with dittus boelter equation and different turbulence model which are

used and compared to see which is in fig.5.2 the difference for suitable results. Turbulence model are selected based on the value of Nusselt number with respect to Reynolds number for both design. K-ε model standard and K-ε model RNG, K-ε model realizable model are used to verify the results. The Nusselt number obtained using Dittus-Boelter eq. for both design As the result of different turbulence models compare with dittus K-ε turbulence RNG model is gives better result its near to study the present work.

For friction factor of smooth duct is calculated by modified blasius equation and compared with CFD result show in fig 5.3 the result varies between 2.4% to 9.6%.

5.2 EFFECT OF RELATIVE ROUGHNESS PITCH

Effect of relative roughness pitch on nusselt no. and friction factor for different Reynolds no range 4000 to 20000. It is known that irrespective of convective heat transfer coefficient is significantly higher in roughened duct as compared with smooth duct. This fact is also evident from the figure and is due to the flow separation and mixing induced by eddies formation in the wake region of each rib. It should be noted that effective roughness pitch at $P/e = 10$. the variation in nusselt no. is due to low heat transfer boundary layer formation on

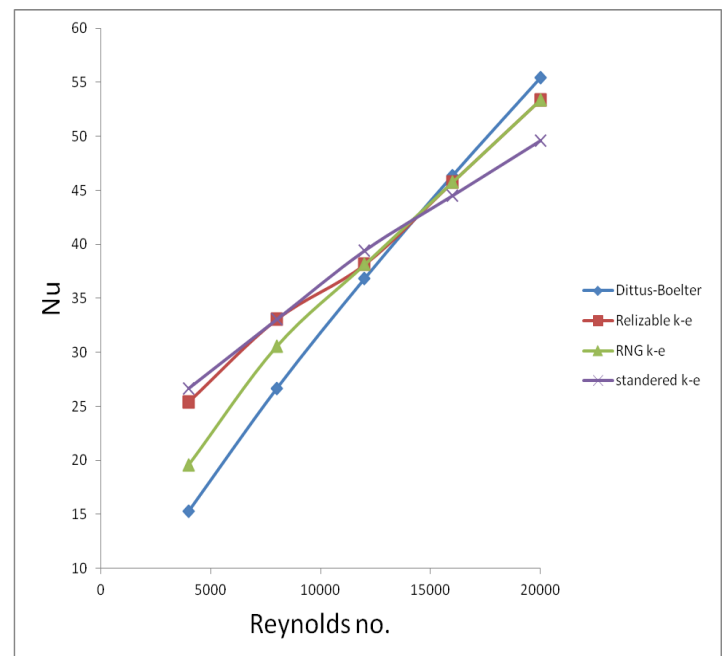


Fig. 4.2 Reynolds number and Nusselt number for different turbulent model.

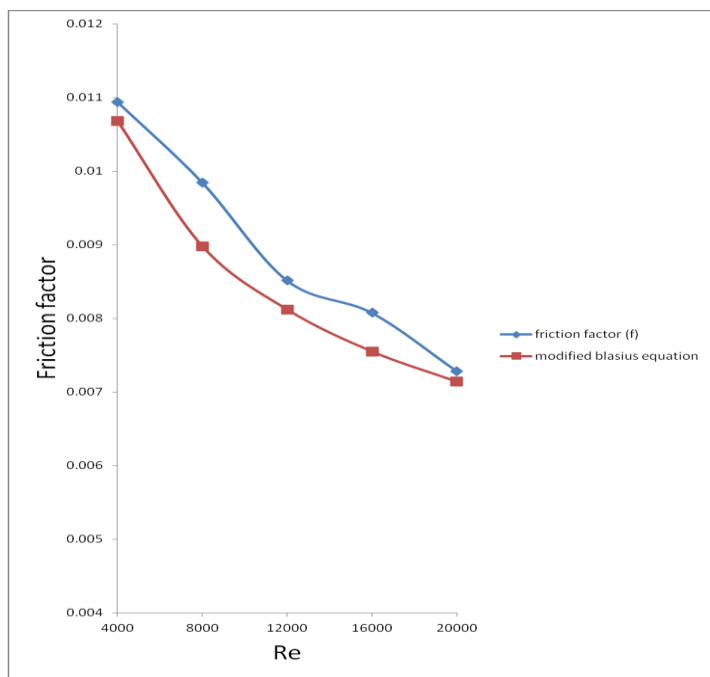


Fig .4.3 Friction factor .and Reynolds no. cfd & modified blasius equation

5.3 EFFECT ON ARC ANGLE

The variation of Nusselt number as function of angle of attack (α) at different values of Reynolds number. Nusselt no. increases with increase in Reynolds no. for different angle 30° , 45° , 60° and 75° . Nusselt no. has maximum at angle of attack at 30° above this vale of angle of attack Nusselt no. decreases for different Reynolds no.

5.4 ENHANCED NUSSELT NUMBER RATIO

Nusselt number enhancement ratio gives information about the increment in Nusselt number of a solar air heater with ribs from that of a smooth one. Fig. 4.8 gives a comparison Nusselt number enhancement with Reynolds no. for different roughness pitch. In this best Nusselt number enhancement ratio. The maximum Nu/Nus values is 2.2524 with $p/e=10$, $\alpha=30^\circ$, $g/e=1$ and $e/Dh=0.045$ is observed at 12000.

5.5 ENHANCED FRICTION FACTOR RATIO

Friction factor enhancement ratio gives information about pressure drop where pressure drop is maximum no extra pumping power is required. In fig.4.9 the maximum value of friction factor ratio is 2.7029 for $p/e=10$, $g/e=1$, $e/Dh=0.045$ and $\alpha=30^\circ$ at Reynolds no.12000.

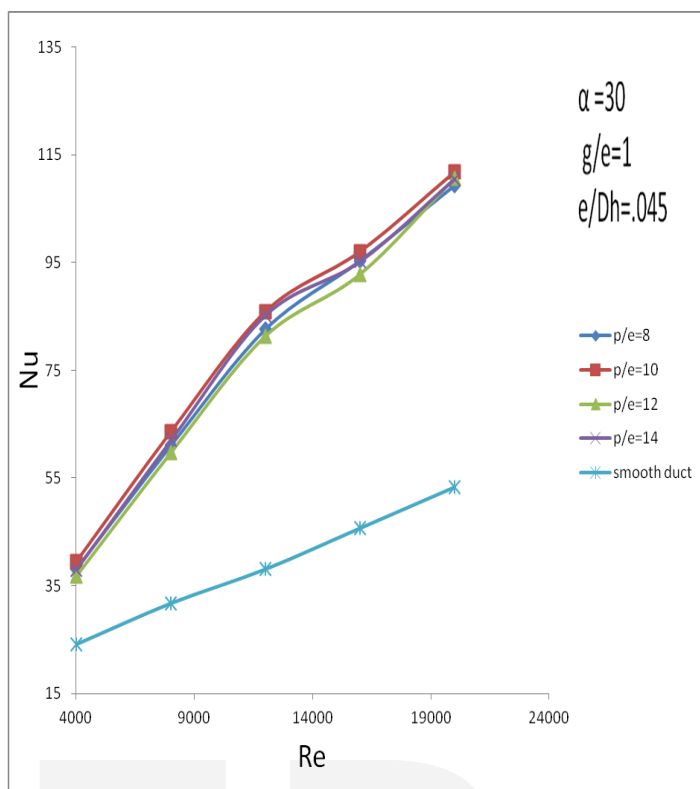


Fig. 4.4 Nusselt Number and Reynolds no. at different roughness pitch

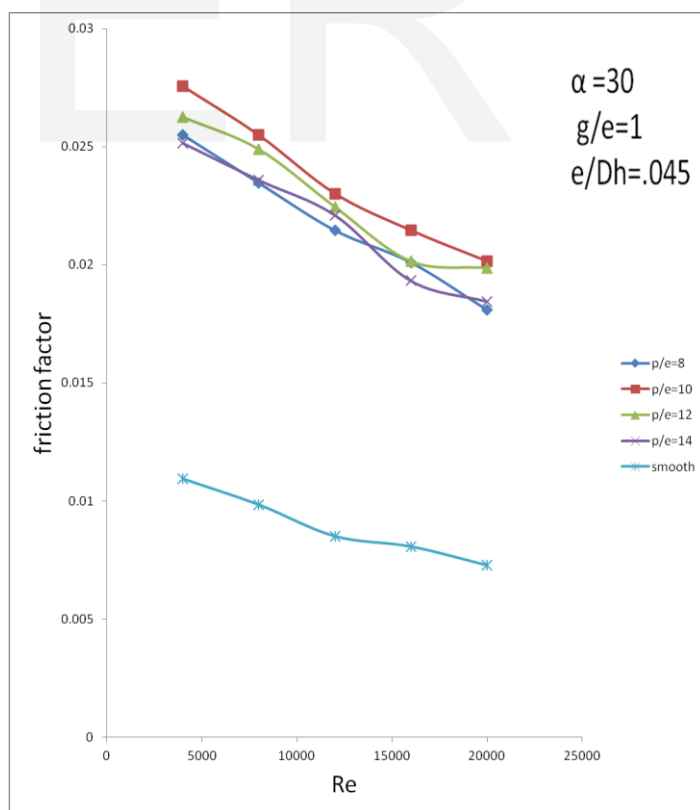


Fig .4.5 Friction Factor and Reynolds no. with different roughness pitch

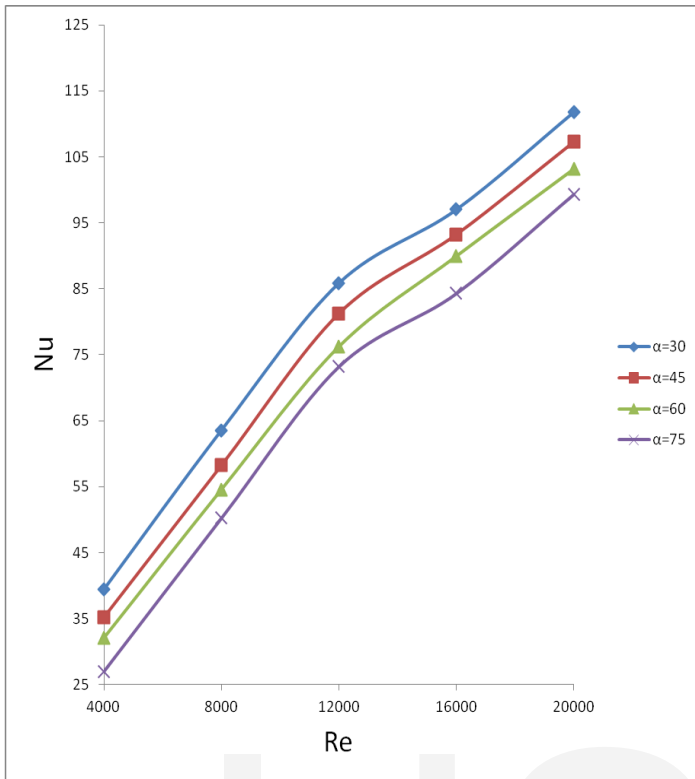


Fig.4.6 Nusselt no. and Reynolds no. for different arc angle

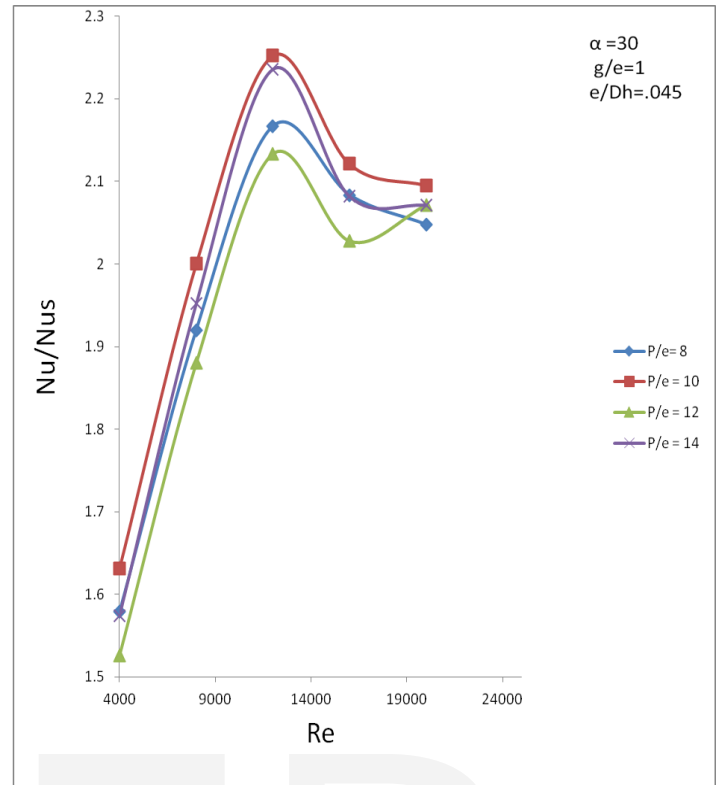


Fig.4.8 Nu/Nus and Reynolds no.

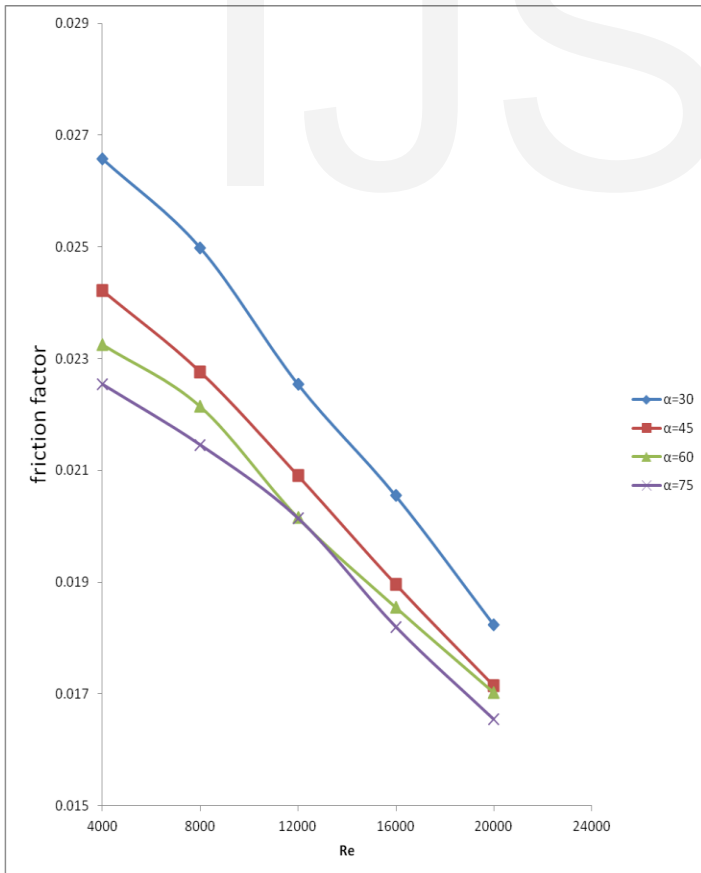


Fig..4.7 Friction factor and Reynolds no.

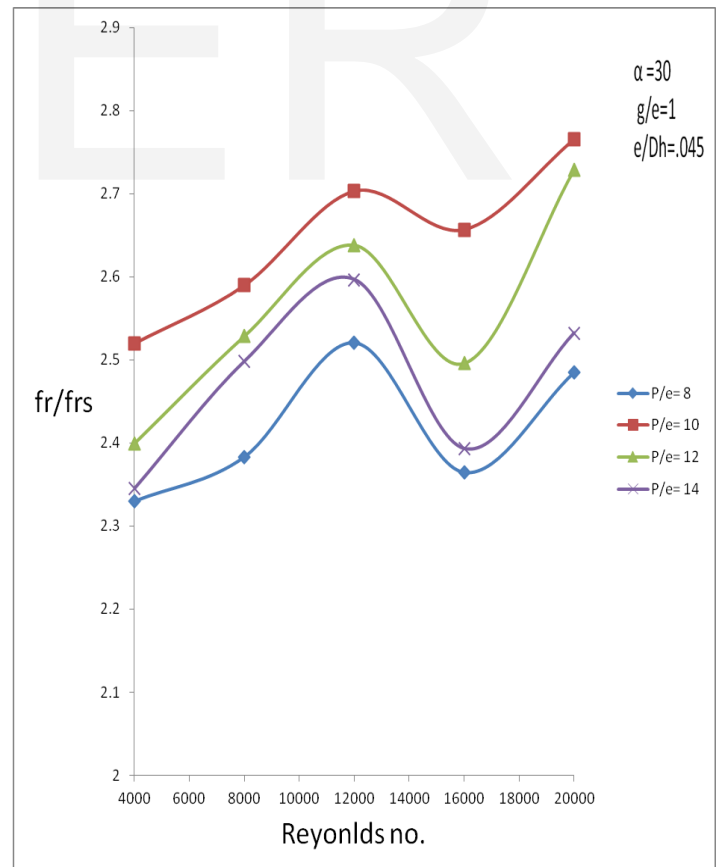


Fig. 4.9 fr / frs and Reynolds no.

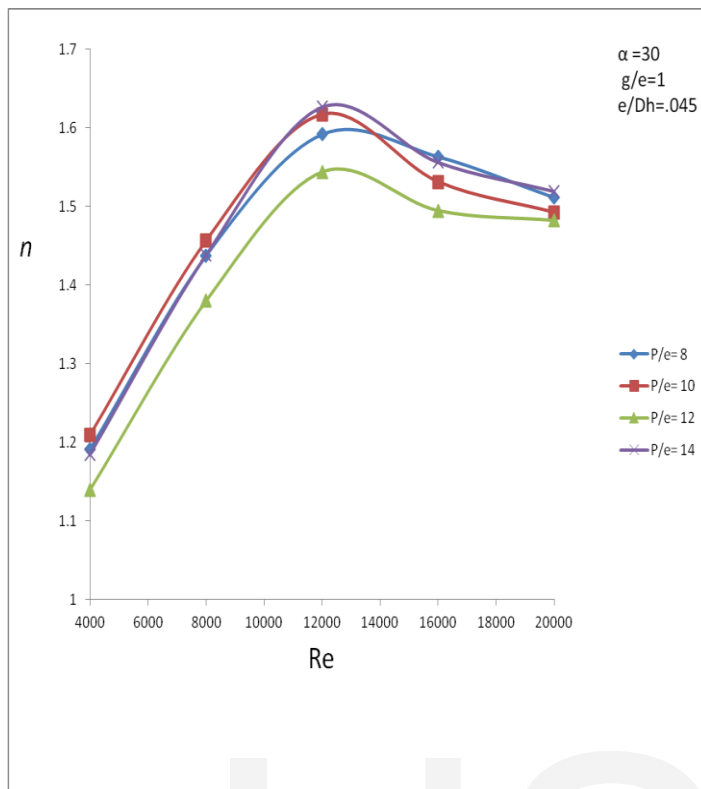


Fig.4.10 Thermohydraulic performance and Reynolds no.

CONCLUSION

In this CFD analysis, operation performed on Ansys Fluent 15.0 the effect of arc shape ribs arranged in Broken curved rib shaped pattern on one of the broad wall of solar air heater duct has been investigated. The effect of the relative roughness width (W/w), relative roughnesspitch (p/e) and relative roughness height (e/Dh) on heat transfer (Nusselt number) and friction factor has been analyzed. Based on this investigation the following conclusions were made.

- i) The average value of Nusselt no. is increased with Reynolds no. increases for all different value of roughness pitch
- ii) The average friction factor decreases with different Reynolds no. for different value of roughness pitch
- iii) The average value of Nusselt no. is decreases with same Reynolds no with increase Arc angle
- iv) Maximum Nusselt no. has been found to be 2.2524 times compared to smooth duct responding to roughness pitch (p/e) 10 , roughness height (e/Dh) 0.045 and arc angle 30° at Reynolds no. 12000 .

v) The value of Thermo-hydraulic Performance Varies between 1.1851 to 1.6267 for to roughness pitch (p/e) 10, roughness height (e/Dh) 0.045 and arc angle 30° at Reynolds no. 4000 to 20000.

vi) Optimum value of Thermo- hydraulic performance is 1.6267 has found at roughness pitch (p/e) 10, roughness height (e/Dh) 0.045 and arc angle 30° at Reynolds no. 12000.

REFERENCES

- [1] V.S. Hans, R.S. Gill, Sukhmeet Singh, "Heat transfer and friction factor correlations for a solar air heater duct roughened artificially with broken arc ribs" (2016).
- [2] Tabish alam, "Numerical study on thermal hydraulic performance improvement in solar air heater duct with semi ellipse shaped obstacles" (2015).
- [3] Tabish alam, "A critical review on artificial roughness provided in rectangular solar air heater duct" (2013)
- [4] Deep Singh Thakur, Mohd. Kaleem Khan, Manabendra Pathak, "Performance Evaluation of Solar Air Heater with Novel Hyperbolic Rib Geometry" (2015).
- [5] Amit Kumar Ahuja, J. L. Bhagoria "A CFD based Thermo-Hydraulic Performance Analysis of an Artificially Roughened Solar Air Heater Having Circular Ribs on the Absorber Plate" n (2015).
- [6] N.K. Pandey, V.K. Bajpai, Varun "Experimental investigation of heat transfer augmentation using multiple arcs with gap on absorber plate of solar air heater" (2016).
- [7] Yadav A.S., Bhagoria J.L., "A CFD based heat transfer and fluid flow analysis of a solar air heater provided with circular transverse wire rib roughness on the absorber plate", Energy, Vol. 55, pp. 1127 - 1142, (2013).
- [8] Raj Kumar et al. "Study and correlation development correlation for Nusselt number and friction factor for discredited broken V-pattern baffle solar air channel"
- [9] Karwa R., Solanki, S. C. and Saini, J. S., "Heat transfer coefficient and friction factor correlations for the transitional flow regime in rib-roughened rectangular ducts", International Journal of Heat and Mass Transfer" 1999.
- [10] Sukhatme K. and Sukhatme S. P., 1996, "Solar energy: principles of thermal collection and storage, Tata McGraw-Hill Education".
- [11] Cengel Y. A. and Cimbala J. M., 2006, "Fluid mechanics (Vol. 1), Tata McGraw-Hill Education".
- [12] Yadav A. S. and Bhagoria J. L., "Heat transfer and fluid flow analysis of solar air heater: a review of CFD approach", Renewable and Sustainable Energy Reviews, 2013
- [13] Kumar A., Bhagoria, J. L. and Sarviya R. M., "Heat transfer and friction correlations for artificially roughened solar air heater duct with discrete W-shaped ribs", Energy Conversion and Management 2009,
- [14] Khushmeet Kumar, D.R. Prajapati, Sushant Samir, Investigation on Heat Transfer and Friction Factor Correlations De-

velopment for Solar Air Heater Duct Artificially Roughened with 'S' Shape Ribs

[15] R.S. Gill, V.S. Hans, J.S. Saini, Sukhmeet Singh, Investigation on performance enhancement due to staggered piece in a broken arc rib roughened solar air heater duct, *Renewable Energy* (2016), doi: 10.1016/j.renene.2016.12.002

[16] Yadav and Bhagoria " A CFD base heat transfer and fluid flow analysis of a solar air heater provided with circular transverse wire rib roughness on the absorber plate." *Renewable energy*, 2013

[17] A review on Solar Air Heater using various artificial roughness geometries Ankit C.Khandelwal, 2Samir A.Dhatkar, 3A.B.Kanas-Pat

[18] Deep Singh Thakur, Mohd. Kaleem Khan, Manabendra Pathak, Performance Evaluation of Solar Air Heater with Novel Hyperbolic Rib Geometry, *Renewable Energy* (2016), doi:10.1016/j.renene.2016.12.092

[19] Jaurker, A.R. Saini, J.S. and Gandhi, B.K., "Heat transfer and friction characteristics of rectangular solar air heater duct using rib-grooved artificial roughness", *Solar Energy*, 80, pp. 895 - 907, (2006).

[20] Karmare, S.V. and Tikekar, A.N., (2007). Heat transfer and friction factor correlation for artificially roughened duct with metal grit ribs, *Int. Journal of Heat Mass Transfer*, 50, pp. 4342 - 4351.

[21] Karwa, R. Solanki, S.C. and Saini, J.S., (1999) Heat transfer coefficient and friction factor correlations for the transitional flow regimes in rib-roughened rectangular duct, *Int. Journal of Heat Mass Transfer*

[22] T. Alam, R.P. Saini, J.S. Saini, Use of turbulators for heat transfer augmentation in an air 15 duct - a review, *Renewable Energy*, 62 (2014), pp. 689-715

[23] Aharwal, Gandhi and saini "Heat transfer and friction characteristics of solar air heater ducts having integral inclined discrete ribs on absorber plate" *Heat and mass transfer* (2009).

[24] Langewar, Bhagoria and Agrawal "Review of development of artificial roughness in solar air heater and performance evaluation of different orientations for double arc rib roughness"

[25] Singh A.P., Varun, Siddhartha, (2014), "Effect of artificial roughness on heat transfer and friction characteristics having multiple arc shaped roughness element on the absorber plate", *Solar Energy*, Vol. 105, pp. 479 - 493.